Noninvasive Assessment of Hemodynamic Status in HeartWare Left Ventricular Assist Device Patients. Validation of an Echocardiographic Approach

Published version:

DOI:10.1016/j.jcmg.2018.01.026

(Article begins on next page)

“Non-invasive Assessment of Hemodynamic Status in HeartWare Left Ventricular Assist Device Patients Validation of an Echocardiographic Approach”

Simone Frea, MD,[a] Paolo Centofanti, MD,[b] Stefano Pidello, MD,[a] Francesca Giordana, MD,[a] Virginia Bovolo, MD,[a] Andrea Baronetto, MD,[b] Beatrice Franco, MD,[a] Marco Matteo Cingolani, MD,[a] Matteo Attisani, MD,[b] Mara Morello, MD,[a] Serena Bergerone, MD,[a] Mauro Rinaldi, MD,[b] Fiorenzo Gaita, MD [a]

[a] Division of Cardiology, Città della Salute e della Scienza University Hospital of Torino, Torino, Italy

[b] Division of Cardiac Surgery, Città della Salute e della Scienza University Hospital of Torino, Torino, Italy

ABSTRACT

Objectives The aim of this prospective study was to validate an echocardiographic protocol derived from 5 HeartWare left ventricular assist device (HVAD) patients for the noninvasive evaluation of right atrial pressure (RAP) and left atrial pressure (LAP) in HVAD patients.

Background Echocardiography is an invaluable tool to optimize medical treatment and pump settings and also for troubleshooting residual heart failure. Little is known about the echocardiographic evaluation of hemodynamic status in HVAD patients.

Methods Right heart catheterization and Doppler echocardiography were performed in 35 HVAD patients. Echocardiography-estimated RAP (eRAP) was assessed using inferior vena cava diameter, hepatic venous flow analysis, and tricuspid E/e′ ratio. Echocardiography-estimated LAP was assessed using E/A ratio, mitral E/e′ ratio, and deceleration time.

Results eRAP and estimated LAP significantly correlated with invasive RAP and LAP (respectively, $r = 0.839$, $p < 0.001$, and $r = 0.889$, $p < 0.001$) and accurately detected high RAP and high LAP (respectively, area under the curve 0.94, $p < 0.001$, and area under the curve 0.91, $p < 0.001$). High eRAP was associated with high LAP (area under the curve 0.92, $p < 0.001$) and correlated with death or hospitalization at 180 days (odds ratio: 8.2; 95% confidence interval: 1.1 to 21.0; $p = 0.04$). According to estimated LAP and eRAP, patients were categorized into 4 hemodynamic profiles. Fifteen patients (43%) showed the optimal unloading profile (normal eRAP and normal wedge pressure). This profile showed a trend toward a lower risk for adverse cardiac events at follow-up (odds ratio: 0.2; 95% confidence interval: 0.1 to 1.0; $p = 0.05$) compared with other hemodynamic profiles.

Conclusions Doppler echocardiography accurately estimated hemodynamic status in HVAD patients. This algorithm reliably detected high RAP and LAP. Notably, high RAP was associated with high wedge pressure and adverse outcome. The benefit of noninvasive estimation of hemodynamic status in the clinical management of patients with left ventricular assist devices needs further evaluation.

Key Words

echocardiography

hemodynamic assessment

HVAD

left atrial pressure

left ventricular assist device

Abbreviations and Acronyms

AUC = area under the curve

DT = deceleration time

eLAP = estimated left atrial pressure

eRAP = estimated right atrial pressure

HVAD = HeartWare left ventricular assist device

IVC = inferior vena cava

LAP = left atrial pressure

LV = left ventricular

LVAD = left ventricular assist device

MR = mitral regurgitation

PAPi = pulmonary artery pulsatility index

RHC = right heart catheterization

RV = right ventricular

RAP = right atrial pressure

sPAP = systolic pulmonary artery pressure

VTI = hepatic venous velocity-time integral

WP = wedge pressure

Left ventricular assist devices (LVADs) are intended to improve cardiac output and unload the left ventricle without excessive overload on the right cardiac chambers 1, 2, 3. Inefficient unloading of the left ventricle may be associated with failure to diminish heart failure symptoms, and right ventricular (RV) performance could be the limiting factor on total cardiac output after LVAD implantation. Echocardiography is an invaluable tool to optimize medical treatment and pump settings and for troubleshooting possible device malfunctions 4, 5, 6, 7, 8, 9. Echocardiographic protocols were prospectively validated in HeartMate II (Thoratec Corporation, Pleasanton, California) LVAD patients 8, 9, 10, 11. However, little is known about echocardiographic evaluation in those with HeartWare (Framingham, Massachusetts) LVADs (HVADs). Therefore, we performed a prospective study to validate a pre-specified echocardiographic protocol for the noninvasive evaluation of hemodynamic status in a selected population of HVAD-implanted patients.

METHODS

Patient population and study design

In this single-center prospective study, all consecutive HVAD patients who underwent right heart catheterization (RHC) between July 2014 and April 2017 were enrolled. Patients underwent RHC to assess or maintain heart transplantation candidacy or for persistent heart failure (12). If no pulse or narrow pulse was present, Doppler blood pressure was measured (13), while pulsatile mean arterial pressure was derived from systolic and diastolic blood pressure. A Doppler blood pressure or mean arterial pressure goal of ≤80 mm Hg was used.

Echocardiographic evaluation was performed by blinded operators (S.F. and M.M.) according to a pre-specified protocol within 60 min before RHC. Follow-up was performed 180 days after RHC.

Adverse outcomes were considered a composite of cardiac death, hospitalization for heart failure, RV mechanical support, or urgent heart transplantation within 180 days of RHC.

The study was drafted according to the Declaration of Helsinki, International Council for Harmonisation of Technical Requirements for Pharmaceuticals for Human Use good clinical practice, and regulatory requirements and was approved by the local Institutional Review Board; patients gave written informed consent.

Echocardiographic measures

Two-dimensional transthoracic echocardiography was performed according to a pre-specified protocol using a Philips i33 machine (Philips Medical Systems, Andover, Massachusetts).

Left ventricular (LV) chamber size and function were measured (14). Inspection and qualitative description of inlet cannula was performed. Aortic regurgitation and mitral regurgitation (MR) were assessed using color Doppler (15). Interventricular septal position and aortic valve opening (16) were evaluated. Right or left shift of the septum was respectively considered a marker of inefficient or excessive unloading (8).

Basal RV end-diastolic diameter, tricuspid annular plane systolic excursion, 2-dimensional RV fractional area change, and tissue Doppler–derived tricuspid lateral annular peak systolic velocity (S′) were measured (17). Tricuspid regurgitation was qualitatively assessed. Transtricuspid systolic gradient was estimated by tricuspid regurgitation peak velocity, and RV contraction-pressure index was derived as tricuspid annular plane systolic excursion × transtricuspid systolic gradient (18). Finally we estimated the pulmonary artery pulsatility index (PAPi) (19) as follows: estimated PAPi = transtricuspid systolic gradient/estimated right atrial pressure (eRAP) (see the following text).

Noninvasive hemodynamic protocol

Derivation cohort

The noninvasive hemodynamic protocol was developed according to the best Doppler echocardiographic knowledge and was previously tested and optimized on a derivation cohort of 5 HVAD patients (patients not included in the study). In this cohort, Doppler echocardiographic estimation of right atrial pressure (RAP) significantly correlated with RAP obtained by RHC ($r = 0.915$, $R^2 = 0.837$, $p = 0.029$). Estimation of left atrial pressure (LAP) according to 2 different models ($eLAP_1$ and $eLAP_2$; see below) showed a trend toward a significant correlation with wedge pressure (WP) (respectively, $r = 0.830$, $R^2 = 0.69$, $p = 0.16$, and $r = 0.794$, $R^2 = 0.630$, $p = 0.11$).

RAP estimation

Expiratory and inspiratory inferior vena cava (IVC) diameters within 2 cm from the right atrium and hepatic vein flow were measured in subcostal views, while peak early transtricuspid inflow velocity and tissue Doppler analysis of tricuspid annular velocities were measured in a right ventricle–focused apical 4-chamber view.

RAP was estimated using IVC diameter and collapse (20), hepatic venous flow pattern (hepatic venous systolic-to-diastolic wave ratio) (21), and hepatic venous systolic filling fraction (ratio of systolic and diastolic hepatic venous velocity-time integrals (VTIs) (systolic VTI/[systolic VTI + diastolic VTI]) (22) and using the tricuspid E/e′ ratio 23, 24 (Figures 1A and 2A to 2D). IVC diameter >2.1 cm, hepatic venous systolic-to-diastolic wave ratio <1, hepatic venous systolic filling fraction < 55%, and tricuspid E/e′ ratio >6 were considered markers of high (>10 mm Hg) RAP. Lower and higher cutoff values of eRAP were derived from the models as follows: RAP = 21.6 − 24 × hepatic venous systolic filling fraction for hepatic vein flow analysis and RAP = 1.62 × E/e′ + 2.13 for tricuspid E/e′ ratio analysis 22, 24. Finally, the conclusive eRAP was the average of RAP values estimated by at least 2 of the 3 aforementioned parameters.

Figure 1. *Doppler Echocardiographic Protocol for Noninvasive Assessment of Right Atrial Pressure and Wedge Pressure*

A $eRAP = (eRAP_{IVC} + eRAP_{HVFF} + eRAP_{right\ E/e'})/3^*$

* or mean of available values

	$eRAP_{IVC}$	$eRAP_{HVFF}$	$eRAP_{right\ E/e'}$
20 mm Hg	IVC > 21 mm without collapse	$V_S < V_D$ and HVFF < 45% or Vs reverse	> 8
15 mm Hg	IVC > 21 mm with < 50% collapse	$V_S < V_D$ and HVFF < 55%	> 6
10 mm Hg	IVC > 21 mm with > 50% collapse OR IVC ≤ 21 mm with < 50% collapse	$V_S < V_D$ and HVFF < 55%	> 4
5 mm Hg	IVC ≤ 21 mm with ≥ 50% collapse	$V_S > V_D$	≤ 4

B $eLAP_2 = (eLAP_{E/A} + eLAP_{MDI} + eLAP_{septal\ E/e'} + eLAP_{MR})/4^*$

* or mean of available values

	$eLAP_{E/A}$	$eLAP_{MDI}$	$eLAP_{septal\ E/e'}$	$eLAP_{MR}$
20 mm Hg	Restrictive (DT < 125 ms)	< 1.5	≥ 20	4+/4+
15 mm Hg	Restrictive (DT 125-160 ms)	< 2	≥ 15	3+/4+
10 mm Hg	Pseudonormal	> 2	≥ 8	2+/4+
5 mm Hg	Impaired relaxation	> 3	< 8	1+/4+

(A) Estimated right atrial pressure (eRAP) results from the mean of eRAP derived from inferior vena cava (IVC), hepatic venous systolic filling fraction (HVFF, [VTIS/(VTIS + VTID)]), and right E/e′ ratio. **(B)** Estimated left atrial pressure (eLAP) results from the mean of eLAP evaluated by diastolic pattern, mitral deceleration index (MDI), septal E/e′, and mitral regurgitation (MR). VTI_D = diastolic velocity-time integral; VTI_S = systolic velocity-time integral.

Figure 2*. Right Atrial Pressure Estimation in a Patient in New York Heart Association Functional Class I With Signs of Heart Failure*

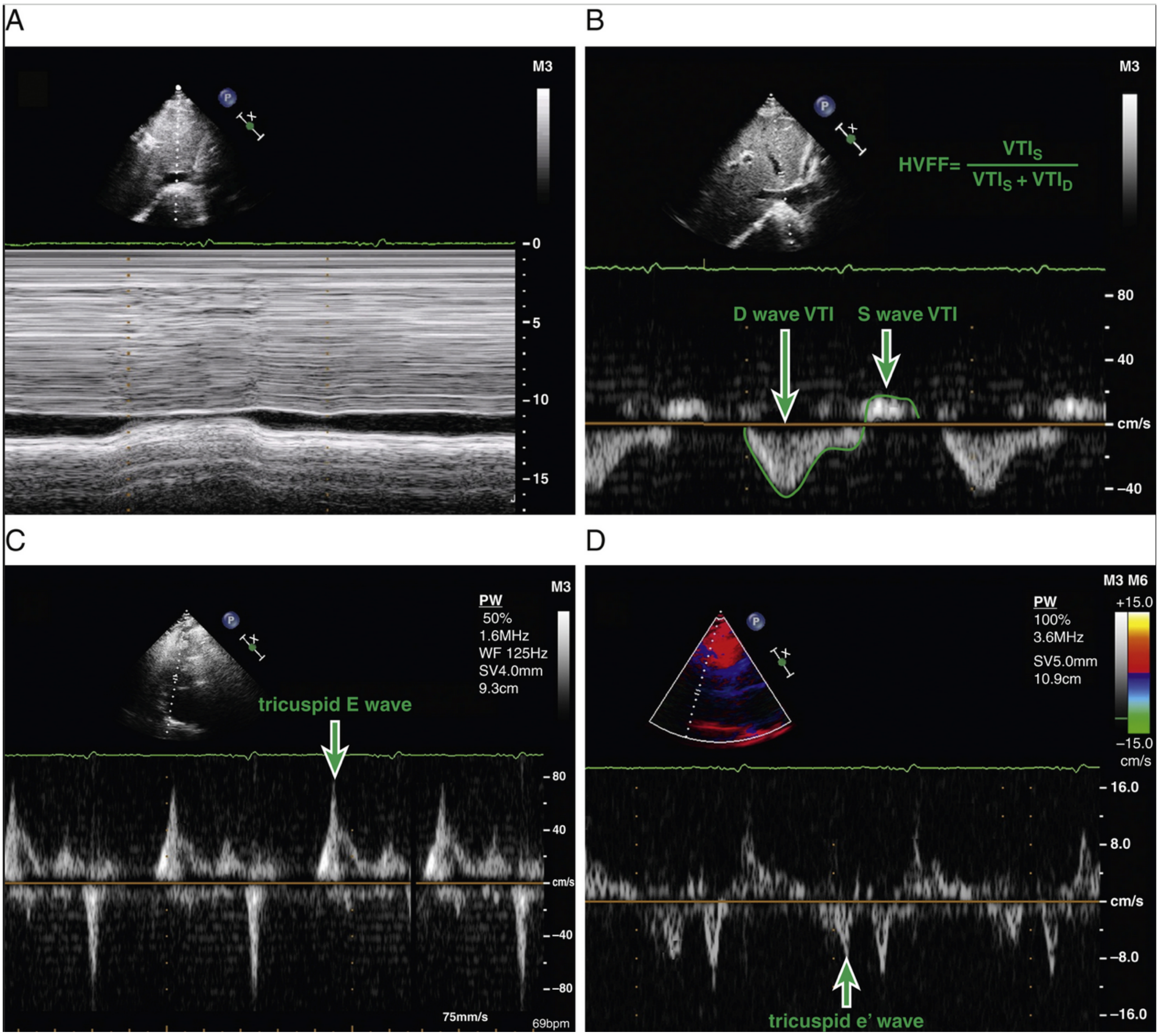

(A) Subxiphoid assessment of inferior vena cava (IVC) diameter: maximum 15 mm and 3 mm after inspiratory collapse → estimated right atrial pressure $(eRAP)_{IVC}$ 5 mm Hg. **(B)** Pulsed-wave Doppler imaging of hepatic veins flow showing reverse S wave, increased D wave → $eRAP_{HVFF}$ 20 mm Hg. **(C, D)** Tricuspid inflow and tricuspid annular e′: E/e′ ratio > 6 → $eRAP_{right\ E/e'}$ 15 mm Hg. eRAP is 13 mm Hg ([5 + 20 + 15]/3). On right heart catheterization, mean RAP was 16 mm Hg. The only use of IVC (a low sensible parameter) would have been misleading, suggesting normal instead of high right atrial pressure. HVFF = hepatic venous systolic filling fraction; VTI_D = diastolic velocity-time integral; VTI_S = systolic velocity-time integral.

LAP estimation

The first estimation of LAP ($eLAP_1$) was derived from eRAP and interatrial septal position. Interatrial septal position was assessed at diastole using the left parasternal short-axis view and/or 4-chamber view 8, 25. $eLAP_1$ was considered equal to eRAP if the interatrial septum position was neutral, while $eLAP_1$ was 5 mm Hg higher or lower if the septum was deviated respectively to the right or to the left side.

The second multiparametric model ($eLAP_2$) used transmitral Doppler analysis (diastolic pattern analysis assessed by E/A ratio and deceleration time [DT] of the E-wave and the mitral deceleration index, as the DT/E-wave peak velocity ratio) (26), tissue Doppler analysis of mitral annular velocities (mitral septal E/e′ ratio), and MR degree, as a direct marker of LV load (Figure 1B). Tricuspid regurgitation peak velocity was not included in the $eLAP_2$ model, because it was independently evaluated as an indirect measure of LAP (27). Pre-specified predictors of high (>15 mm Hg) WP were a restrictive filling pattern (E/A ≥2 and DT <160 ms), a mitral deceleration index <2 ms/(cm/s), a septal E/e′ ratio ≥15 (28), MR ≥3+/4+, or diastolic MR and a tricuspid regurgitation peak velocity >2.8 m/s. Finally, the conclusive $eLAP_2$ value was the average of the eLAP values estimated by the 4 (or fewer if 1 or more parameters were not available) aforementioned parameters.

A third model for the detection of high LAP, proposed by Estep et al. (9) and including E/A ratio, RAP assessed by IVC diameter and hepatic venous flow, systolic pulmonary artery pressure (sPAP), E/e′ ratio, and left atrial volume index, was used.

Finally, according to $eLAP_2$ and eRAP, patients were classified into 4 different hemodynamic profiles: optimal unloading (normal eLAP and eRAP), RV failure (normal eLAP and high eRAP), LV failure (high eLAP and normal eRAP), and biventricular failure (high eLAP and high eRAP).

Cardiac catheterization

RHC was performed in our catheterization laboratory by an operator blinded to all Doppler echocardiographic data. RAP, pulmonary artery pressure, and mean WP were measured; cardiac output was derived. Mean WP was considered high when >15 mm Hg and RAP when >10 mm Hg. To evaluate RV function, we calculated RV stroke work index, PAPi ([sPAP − diastolic pulmonary artery pressure]/mean RAP), and the mean RAP/mean WP ratio. To assess RV load, we evaluated pulmonary vascular resistance and the effective arterial elastance (29) as sPAP/SVI.

Statistical analysis

Continuous variables are expressed as mean ± SD and were compared using analysis of variance. Categorical variables are presented as counts and percentages and were compared using the chi-square test. The correlations between variables were evaluated using the Pearson or Spearman rho test and were graphically appraised according to Bland-Altman methods. The same tests were used to evaluate interobserver and intraobserver variability.

Correlations between variables and high LAP or RAP were tested in cross tabulation tables using the Fisher exact test and the Student's *t* test for categorical and continuous variables, respectively.

Receiver-operating characteristic curves were produced to test the abilities of the variables to predict high left and right filling pressures.

Kaplan-Meier curves were used to measure freedom from adverse clinical events according to different noninvasive hemodynamic profiles.

A 2-sided p value <0.05 was considered to indicate statistical significance. All analyses were performed using SPSS version 20.0 (IBM, Armonk, New York).

RESULTS

Baseline characteristics

Thirty-five HVAD patients (mean age 56.9 ± 10.5 years, mean 16 ± 12 months with HVAD support [range 3 to 48 months]) who underwent RHC (24 patients for heart transplantation candidacy and 11 for heart failure) were consecutively enrolled. At HVAD implantation 30 patients had an INTERMACS (Interagency Registry for Mechanically Assisted Circulatory Support) profile ≤3. Table 1 summarizes the characteristics of the population at RHC. Most patients (n = 23 [66%]) were implanted with a “bridge to transplantation” or “bridge to candidacy” indication.

Table 1. Baseline Characteristics (n = 35)

Clinical characteristics	mean ± SD or n (%)
Months on HVAD	15.8 ± 11.6
NYHA functional class ≥III	7 (20.0)
DOBP or MAP, mm Hg	79.6 ± 9.3
Heart rate, beats/min	73.4 ± 12.0
HVAD speed, rates/min	2,497 ± 92
Beta-blockers	35 (100.0)
ACE inhibitors	24 (68.7%)
Furosemide, mg/day	63 ± 62
Adverse cardiac outcome	8 (22.8)
Serum creatinine, mg/dl	1.31 ± 0.51
Total bilirubin, mg/dl	1.09 ± 0.77
Albumin, g/dl	3.67 ± 0.63
Right heart catheterization	
Cardiac index, l/min/m^2	2.06 ± 0.47
mWP, mm Hg	17.8 ± 7.7
sPAP, mm Hg	41.2 ± 12.1
PVR, Wood units	2.04 ± 1.24
mRAP, mm Hg	10.1 ± 4.9
PAPi	2.9 ± 1.5
RVSWI, mm Hg/l · m^2	0.59 ± 0.23
Doppler echocardiographic parameters	
LV ejection fraction, %	18.2 ± 4.4
LV end-diastolic diameter, mm	68.7 ± 10.6
RV/LV diameter ratio	0.63 ± 0.14
Ventricular septum to left	5 (14.2)
Atrial septum to right	6 (17.1)
Aortic valve closed	14 (40.0)
LAVi, ml/m^2	56.9 ± 18.4
MR ≥3+/4+	8 (22.8)
Deceleration time, ms	161.3 ± 64.5
MDI, ms/(cm/s)	2.8 ± 1.7

Septal E/e′ ratio	14.4 ± 6.0
sPAP, mm Hg	39.2 ± 10.1
TAPSE, mm	13.3 ± 2.4
RV S′ peak velocity	7.0 ± 1.9
FAC, %	30 ± 4.6
TR ≥3+/4+	7 (20.0)
eRAP, mm Hg	11.0 ± 4.4

ACE = angiotensin-converting enzyme; DOBP = Doppler blood pressure; eRAP = estimated right atrial pressure; eRAP = estimated right atrial pressure; FAC = fractional area change; HVAD = HeartWare left ventricular assist device; LAVi = left atrial volume index; LV = left ventricular; MAP = mean arterial pressure; MDI = mitral deceleration index; MR = mitral regurgitation; mRAP = mean right atrial pressure; mWP = mean pulmonary capillary wedge pressure; NYHA = New York Heart Association; PAPi = pulmonary artery pulsatility index; PVR = pulmonary vascular resistance; RV = right ventricular; RVSWI = right ventricular stroke work index; sPAP = systolic pulmonary artery pressure; TAPSE = tricuspid annular plane systolic excursion; TR = tricuspid regurgitation.

Clinical outcomes

At 180 days from RHC, 8 patients (23%) experienced adverse outcomes (7 were hospitalized for heart failure, and 1 died of RV failure). Six patients (17%) had clinically relevant suction episodes. Two patients needed aortic valve surgery because of severe aortic regurgitation with cardiogenic shock. Four patients (11%) underwent elective heart transplantation during overall follow-up.

Hemodynamic findings

The enrolled population showed a good range of values at RHC (WP, median 15.5 mm Hg [range 4 to 34 mm Hg]; RAP, median 10 mm Hg [range 3 to 24 mm Hg]). Main hemodynamic characteristics are listed in Table 1. Sixteen patients (46%) showed high WP.

Doppler echocardiographic findings

Main Doppler echocardiographic data are summarized in Table 1. Two patients showed severe aortic regurgitation.

RAP estimation and detection of elevated RAP

Average eRAP was 11.1 ± 4.3 mm Hg (median 12 mm Hg; range 3 to 18 mm Hg). RAP estimated by IVC, tricuspid E/e′ ratio, and hepatic vein hepatic venous systolic-to-diastolic wave ratio correlated significantly with invasive RAP (Table 2). Hepatic vein flow analysis was the most accurate. Multiparametric eRAP showed the highest correlation with invasive RAP (r = 0.839, R^2 = 0.704; mean difference 0.8 ± 3.0, Student's *t* test for mean difference different from zero, p = 0.12) (Figures 3A and 3C) and the greatest diagnostic accuracy (area under the curve [AUC]: 0.94, p < 0.001).

Table 2. Correlation of Echocardiographic Right Atrial Pressure With Invasive Right Atrial Pressure and Detection of High (>10 mm Hg) Right Atrial Pressure

Linear Correlation With RAP					Estimation of RAP >10 mm Hg				
	Patients With Satisfactory Doppler Echocardiographic Signal (n = 35)	r	R^2	p Value		AUC (95% CI)	p Value	Sensitivity	Specificity
Tricuspid E/e′ ratio	30	0.633	0.401	<0.001	Tricuspid E/e′ >6	0.77 (0.59–0.95)	0.01	75.0%	88.6%
Vs/Vd ratio	30	−0.776	0.602	<0.001	Vs < Vd and HVFF <55%	0.93 (0.83–1.00)	<0.001	93.3%	93.3%
IVC maximal diameter	35	0.751	0.564	<0.001	IVC diameter >21 mm	0.78 (0.62–0.94)	0.01	55.6%	100%
$eRAP_{model}$	35	0.839	0.704	<0.001	$eRAP_{model}$ >10 mm Hg	0.94 (0.85–1.00)	<0.001	94.4%	94.1%

AUC = area under the curve; CI = confidence interval; HVFF = hepatic vein filling fraction; IVC = inferior vena cava; RAP = right atrial pressure; tricuspid E/e′ ratio = early tricuspid inflow peak velocity to early annular diastolic peak velocity; Vs/Vd ratio = hepatic vein peak systolic to diastolic wave ratio.

Figure 3. *Correlation Between Doppler Echocardiography and Right Heart Catheterization*

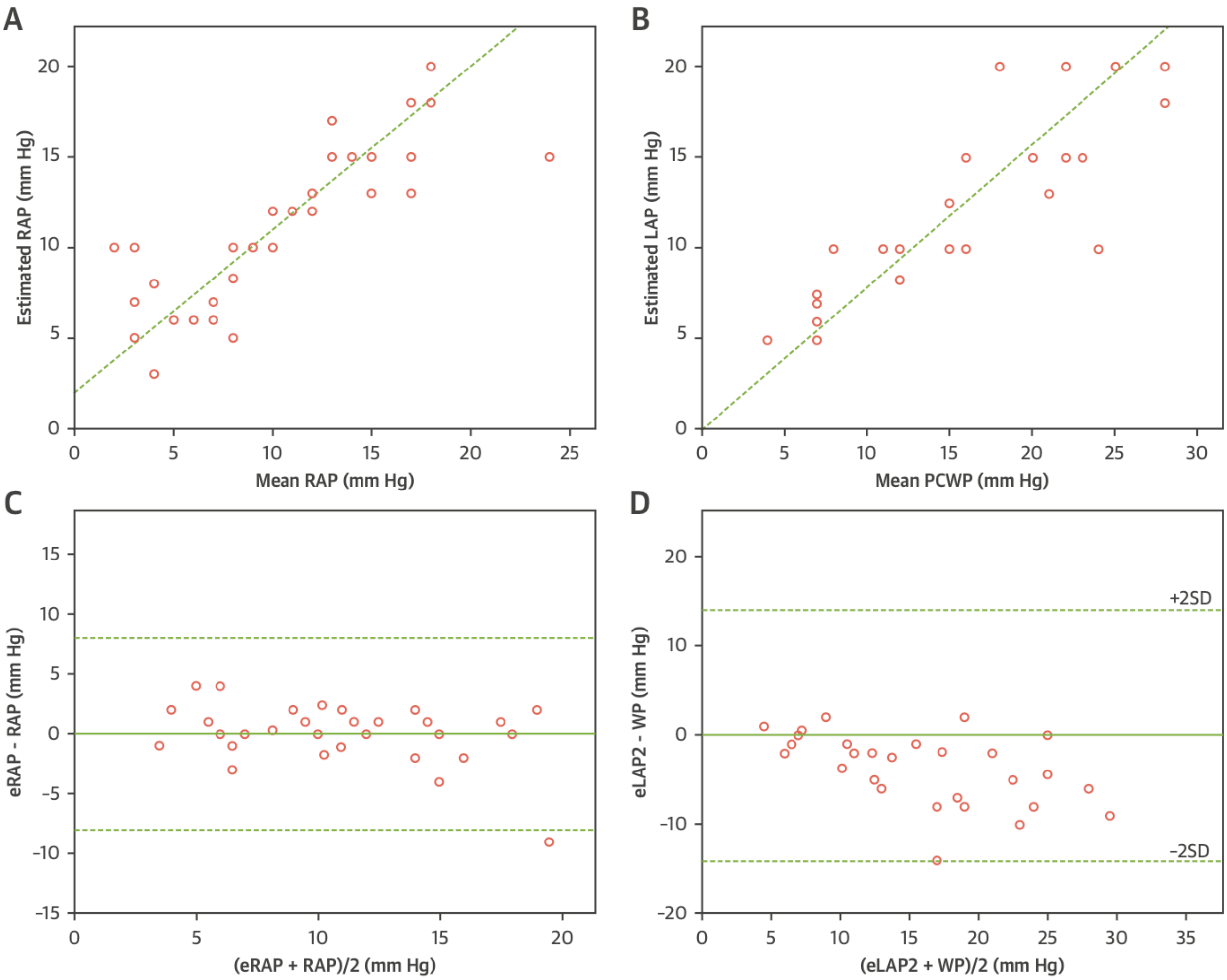

(A) Correlation between estimated right atrial pressure (eRAP) and right atrial pressure (RAP) at right heart catheterization (RHC). **(B)** Correlation between estimated left atrial pressure (eLAP) and wedge pressure (WP) on RHC. **(C)** Bland-Altman plot showing good estimation of RAP by eRAP. **(D)** Bland-Altman plot showing fair estimation of WP by $eLAP_2$ with underestimation for WP higher than 20 mm Hg. PCWP = pulmonary capillary wedge pressure.

LAP estimation and detection of elevated LAP

Patients with high WP showed lower mitral deceleration index (1.71 ± 0.57 ms/[cm/s] vs. 3.67 ± 1.65 ms/[cm/s]; $p < 0.01$), higher septal E/e′ ratio (18.5 ± 4.4 vs. 10.2 ± 4.0; $p < 0.001$), and shorter DT (125.1 ± 33.4 ms vs. 169.3 ± 75.6 ms; $p = 0.04$), while left atrial volume index showed no difference. No patient in the high WP group showed interventricular septum deviated to left, while 5 in the normal WP group did ($p < 0.05$), 4 of whom underwent clinically relevant suction episodes during follow-up (odds ratio: 38; $p < 0.01$). No significant difference in aortic valve opening status was found. The $eLAP_1$ model showed a good correlation with WP (Table 3). This result was driven by eRAP. The $eLAP_2$ model correlated well with high WP (AUC: 0.90; $p < 0.001$), though it underestimated WP higher than 20 mm Hg (mean difference 3.7 ± 3.6, Student's *t* test for mean difference different from zero; $p < 0.01$) (Figures 3B and 3D). The eLAP model of Estep et al. (9) was also a fair predictor of high WP in our setting of patients (AUC: 0.73; p = 0.04). However eLAP according to Estep et al. showed lower specificity. This result was driven mainly by left atrial volume index.

Table 3. Correlation of Echocardiographic Left Atrial Pressure With Wedge Pressure and Detection of High (>15 mm Hg) Wedge Pressure

Linear Correlation With WP					Estimation of WP >15 mm Hg				
	Patients With Satisfactory Doppler Echocardiographic Signal (n = 35)	**r**	**R^2**	**p Value**		**AUC (95% CI)**	**p Value**	**Sensitivity**	**Specificity**
eRAP	35	0.673	0.453	<0.001	eRAP >10 mm Hg	0.92 (0.81–1.00)	<0.001	94.1%	88.9%
IAS position	31	−0.224	0.050	0.21	IAS to the right	0.51 (0.46–0.87)	0.65	33.3%	66.6%
$eLAP_1$	31	0.826	0.682	<0.001	$eLAP_1$ >15 mm Hg	0.83 (0.68–0.99)	0.001	67.8%	100%
MR degree	32	0.585	0.342	<0.001	MR ≥3+/4+	0.63 (0.44–0.83)	0.19	37.5%	88.9%
Diastolic pattern	28	0.754	0.568	<0.001	Restrictive pattern	0.81 (0.64–0.97)	0.01	83.3%	87.8%
Septal E/e′	31	0.763	0.582	<0.001	Septal E/e′ ≥15	0.79 (0.63–0.97)	0.01	76.7%	82.4%
MDI	27	−0.839	0.704	<0.001	MDI <2	0.81 (0.64–0.99)	0.01	75.0%	87.5%
$eLAP_2$	31	0.889	0.790	<0.001	$eLAP_2$ >15 mm Hg	0.91 (0.80–1.00)	<0.001	82.4%	100%
TRV	30	0.646	0.417	<0.001	TRV >2.8 m/s	0.76 (0.57–0.94)	0.02	64.3%	86.7%
LAVi, ml/m^2	35	−0.128	0.016	0.46	LAVi >33 ml/m^2	0.44 (0.25–0.63)	0.55	88.2%	0%
$eLAP_{Estep}$	31	0.433	0.187	0.01	$eLAP_{Estep}$ >15 mm Hg	0.73 (0.54–0.92)	0.04	84.6%	61.1%
eLAP Estep modified	35	—	—	—	eLAP Estep modified >15 mm Hg	0.97 (0.91–1.00)	<0.001	94.1%	100%

eLAP = estimated left atrial pressure; IAS = interatrial septum; TRV = tricuspid regurgitation velocity; WP = mean pulmonary capillary wedge pressure; other abbreviations as in Tables 1 and 2.

Finally, we performed a post hoc analysis. We modified the algorithm proposed by Estep et al. (9) to elaborate a more accurate and practice algorithm (the "Estep modified" model). It was a 2-step algorithm. Multiparametric estimation of RAP was the first step. Afterward, eLAP was assessed using eRAP, E/A, and E/e′ (Figure 4). This brief model allowed a noninvasive estimation of hemodynamic status in all patients with excellent accuracy (AUC for high WP: 0.97).

Figure 4*. Simplified Algorithm for Noninvasive Assessment of Right Atrial Pressure and Wedge Pressure: The "Estep Modified" Model*

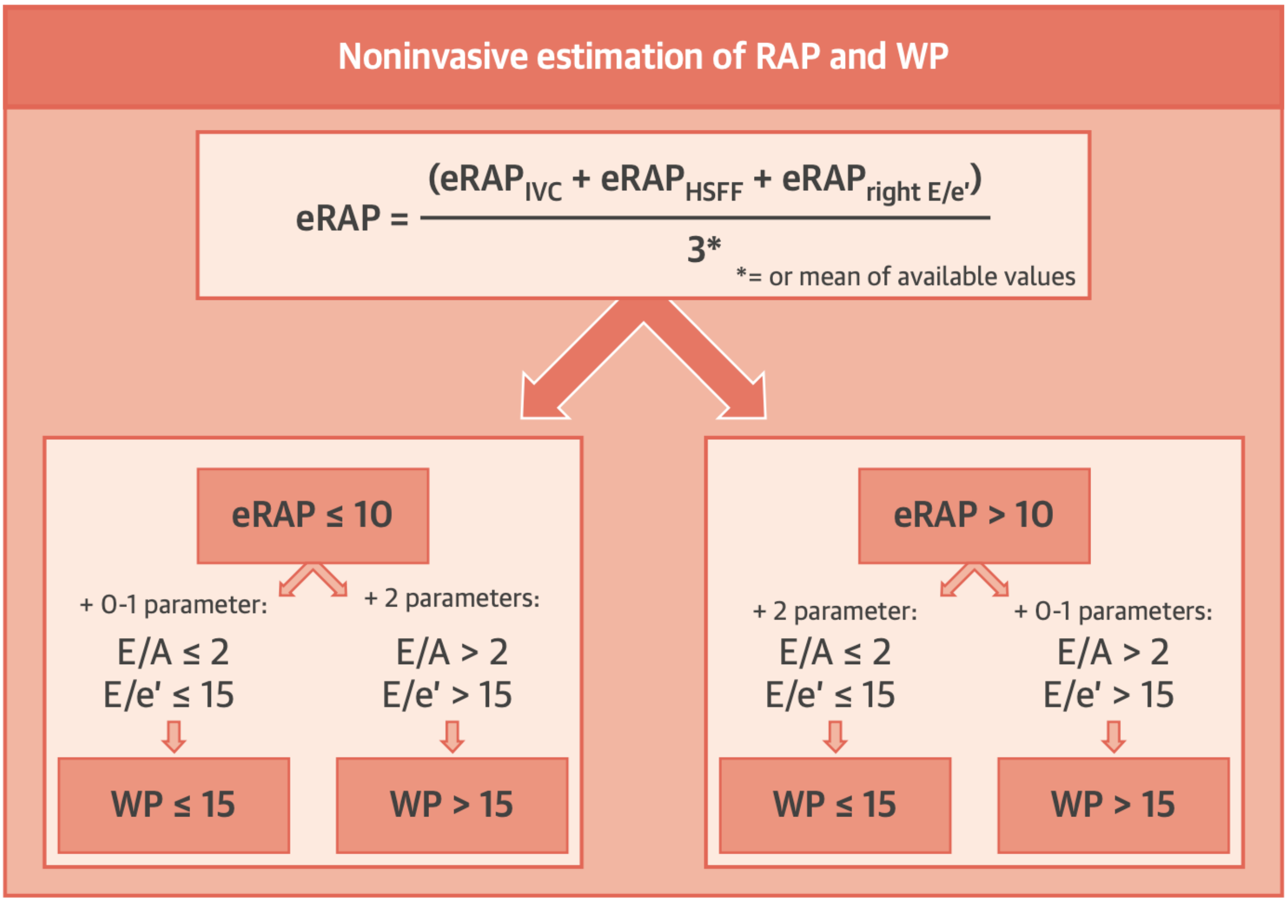

The first step is the estimation of right atrial pressure. The second is the estimation of left atrial pressure by estimated right atrial pressure (eRAP), E/A ratio, and E/e′ ratio. HSFF = hepatic venous systolic filling fraction; IVC = inferior vena cava; WP = wedge pressure.

Doppler echocardiographic estimation of pulmonary hemodynamic status and RV function

There was a good correlation between Doppler echocardiographic estimation of sPAP and sPAP on RHC ($r = 0.728$, $p < 0.001$). Among noninvasive parameters of RV function, Doppler echocardiographic PAPi and eRAP/$eLAP_2$ correlated significantly with invasive PAPi and RAP/WP ($r = 0.581$, $p = 0.002$, and $r = 0.488$, $p = 0.01$, respectively).

Noninvasive hemodynamic profiles

According to eLAP and eRAP, patients were eventually categorized into hemodynamic profiles. Clinical, Doppler echocardiographic, and invasive data according to hemodynamic profiles are shown in Table 4. Fifteen patients (43%) showed the optimal unloading profile, 14 patients (40%) the biventricular failure profile, 1 the LV failure profile, and 5 (14%) the RV failure profile. Compared with the optimal unloading group, the other 2 groups showed worse RV function on RHC, as indicated by PAPi and the mean RAP/mean WP ratio. In particular, the RV failure group showed low-load RV dysfunction (lower sPAP, RV–right atrial gradient, pulmonary vascular resistance, and arterial elastance), while the biventricular failure group showed high-load RV dysfunction (higher sPAP, RV–right atrial gradient, pulmonary vascular resistance, and arterial elastance). Notably, patients with the optimal unloading profile showed a lower risk for adverse cardiac events at follow-up (odds ratio: 0.2; 95% confidence interval: 0.1 to 1.0; $p = 0.05$) (Figure 5) compared with other profiles. In contrast, high eRAP significantly predicted adverse outcomes (odds ratio: 8.2; 95% confidence interval: 1.1 to 21.0; $p = 0.04$).

Table 4. Characteristics by Noninvasive Hemodynamic Profile

	Optimal Unloading (n = 15)	RV Failure (n = 5)	BiV/LV Failure (n = 15)	p Value
Clinical characteristics	n (%) or mean ± SD			
NYHA functional class ≥III	1 (6.6)	2 (40.0)	4 (26.7)	0.19
DOBP or MAP, mm Hg	77.8 ± 5.8	72.2 ± 7.1	83.1 ± 12.5	0.07
Uncontrolled blood pressure	4 (26.6)	1 (20.0)	5 (33.3)	0.82
HVAD speed, rates/min	2515 ± 82	2550 ± 75	2468 ± 127	0.24
ACE inhibitors	11 (73.3)	3 (60.0)	10 (66.6)	0.84
Daily furosemide dose, mg/day	46.0 ± 41.2	65.0 ± 51.8	82.4 ± 72.9	0.24
Time on HVAD, months	12.8 ± 8.0	21.0 ± 15.6	18.9 ± 12.3	0.22
INTERMACS at HVAD implantation (n = 7)	3.6 ± 0.8	2.2 ± 0.4	2.7 ± 0.5	<0.001
Adverse outcome at 180 days	1 (6.7)	3 (60.0)	4 (26.7)	0.04
Hospitalization for heart failure	1 (6.7)	2 (40.0)	4 (26.7)	0.19
Clinical suction	1 (6.7)	3 (60.0)	2 (13.3)	0.02
Elective heart transplantation	1 (6.7)	0 (0.0)	3 (20.0)	0.35
Doppler echocardiographic parameters				
LV end-diastolic diameter, mm	68.2 ± 11.9	62.4 ± 8.7	68.8 ± 7.5	0.44
RV end-diastolic diameter, mm	41.6 ± 6.6	41.4 ± 4.3	45.1 ± 7.7	0.33
RV/LV diameter ratio	0.66 ± 0.16	0.68 ± 0.15	0.60 ± 0.13	0.42
Ventricular septum to left	3 (20.0)	1 (20.0)	0 (0.0)	0.18
Aortic valve closed	7 (46.6)	1 (20.0)	6 (40.0)	0.57
MR (n+/4+)	1.3 ± 1.2	1.0 ± 1.0	2.3 ± 1.2	0.04
sPAP, mm Hg	31.7 ± 4.9	34.3 ± 4.9	46.9 ± 6.6	<0.001
TAPSE, mm	13.5 ± 2.7	12.6 ± 2.6	14.1 ± 2.5	0.52
TR (n+/4+)	1.2 ± 0.6	1.4 ± 1.5	2.3 ± 1.1	0.01
VA gradient, mm Hg	25.5 ± 4.8	20.6 ± 4.5	31.5 ± 5.8	<0.001
RV S’ peak velocity, cm/s	6.4 ± 1.2	8.2 ± 1.3	7.6 ± 2.2	0.07

FAC, %	29.7 ± 4.8	31.0 ± 2.2	30.5 ± 5.3	0.83
RVCPI, mm · mm Hg	346.9 ± 99.3	278.0 ± 119.8	451.6 ± 92.8	0.01
Right heart catheterization				
Cardiac index, l/min/m^2	2.43 ± 0.35	2.54 ± 0.51	2.51 ± 0.34	0.77
mWP, mm Hg	11.4 ± 3.5	15.4 ± 7.9	23.3 ± 5.3	<0.001
mRAP, mm Hg	6.2 ± 2.4	13.2 ± 1.8	13.4 ± 4.1	<0.001
sPAP, mm Hg	33.3 ± 7.1	34.0 ± 8.5	54.9 ± 10.1	<0.001
PAPi	3.7 ± 2.0	1.6 ± 0.4	2.5 ± 0.8	0.01
PVR, Wood units	2.0 ± 0.9	0.8 ± 0.2	2.2 ± 1.5	0.08
Ea, mm Hg/ml	0.99 ± 0.3	1.05 ± 0.25	1.82 ± 0.69	<0.001
mRAP/mWP	0.52 ± 0.22	1.34 ± 1.30	0.63 ± 0.18	0.01
RVSWI, mm Hg/l · m^2	0.51 ± 0.23	0.33 ± 0.29	0.69 ± 0.13	<0.001

BiV = biventricular; Ea = arterial elastance; RVCPI = right ventricular contraction-pressure index; VA gradient = right ventricular–right atrial pressure gradient; Vs/Vd ratio = hepatic vein systolic to diastolic wave ratio; other abbreviations as in Tables 1 and 2.

Figure 5. *Adverse Outcome–Free Survival by Hemodynamic Profiles*

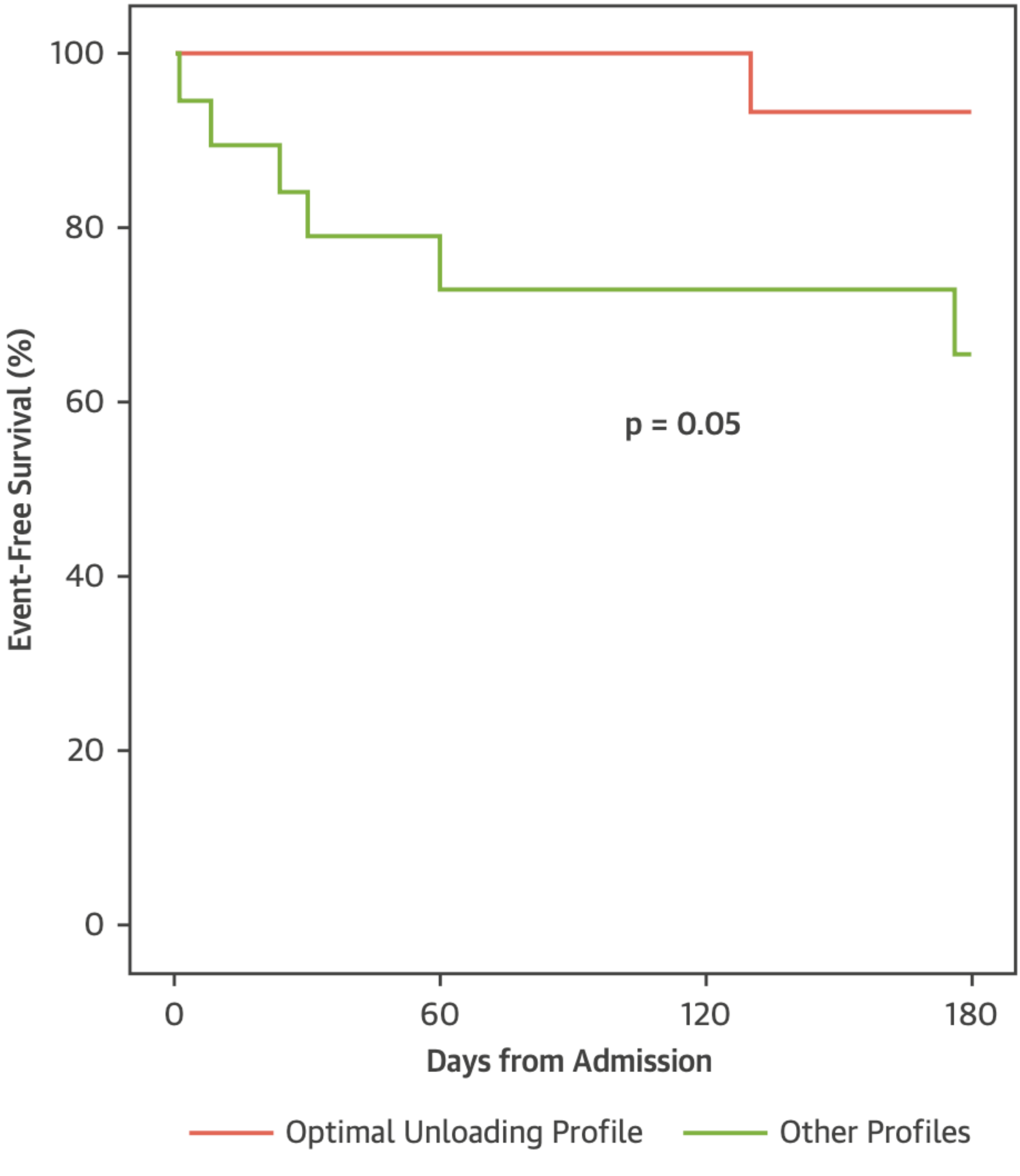

Adverse outcome was a composite of hospitalization for heart failure, death, or urgent heart transplantation. Optimal unloading profile showed a better outcome than other profiles (odds ratio: 0.20; $p = 0.05$).

Reproducibility of echocardiographic parameters

The reproducibility of Doppler echocardiographic and tissue Doppler imaging measurements in our laboratory was previously reported (30). Intraobserver (eRAP: $r = 0.999$, $p = 0.001$; $eLAP_2$: $r = 0.986$, $p = 0.001$) and interobserver (eRAP: $r = 0.994$, $p = 0.001$; $eLAP_2$: $r = 0.931$, $p = 0.001$) estimation of eRAP and $eLAP_2$ showed a very good agreement between measurements.

DISCUSSION

This is the first prospective study to report on the noninvasive Doppler echocardiographic evaluation of hemodynamic status in HVAD patients. We validated a pre-specified protocol for the noninvasive detection of high RAP and LAP.

Estimation of RAP and LAP

The good correlation between IVC and RAP was comparable with that observed in patients without LVADs. Nevertheless, though very specific, a dilated IVC showed low sensitivity in the detection of high RAP. Previous reports suggested that IVC should not be used alone for a reliable estimation of RAP because of its variability and overlap between patients with normal RAP and those with mildly elevated RAP 31, 32. In this respect, hepatic vein flow analysis showed very good sensitivity and diagnostic accuracy, as previously reported (9). The multiparametric approach showed the best accuracy, as it increased sensitivity without affecting specificity.

Despite inlet cannula artifacts, using off-axis views, an adequate mitral pulsed and tissue Doppler analysis of diastolic pattern was reliably obtained in the majority of patients. As previously reported by Estep et al. (9) in HeartMate II–assisted patients, pulsed and tissue Doppler showed a fair linear correlation with WP, and a multiparametric evaluation showed better diagnostic accuracy than single parameters. This suggests that the noninvasive assessment of hemodynamic status is accurate and reproducible and that it is probably not affected by the type of continuous-flow LVAD.

We believe that our study, in addition to that of Estep et al. (9), confirms that noninvasive estimation of hemodynamic status in LVAD patients is accurate and reproducible. In fact, most of our results were similar to those of Estep et al. (9). However, the $eLAP_2$ model showed a better accuracy than that of Estep et al. This was due to the low diagnostic accuracy of left atrial volume.

In fact, in our cohort, almost all patients had severely dilated left atria independent of WP, and this led to an overestimation of high WP. In addition, our results confirmed the strong association between high eRAP and high WP found by Estep et al. (9), as the majority of patients with high WP showed high eRAP. This probably depends on a worsening of RV adaptation to load with LVAD support, as suggested Houston et al. (33).

Moreover, high eRAP was the strongest predictor of adverse outcomes. In this respect, the estimation of RAP should be the first step in the evaluation because of its prognostic value and its diagnostic accuracy. We therefore developed a post hoc 2-step simplified model (the Estep modified model) whose first step is the multiparametric assessment of eRAP. Afterward, WP is assessed. This easier approach focuses on the interplay between the LVAD and the right ventricle (see the following text).

RV function

In line with previous studies, RV function was not captured by conventional Doppler echocardiographic parameters (tricuspid annular plane systolic excursion, fractional area change, and S′ peak velocity), while direct or indirect RV hemodynamic evaluation (PAPi, RV stroke work index, RV contraction-pressure index, RV–right atrial gradient) did. In this regard, the RV failure subgroup showed primary severe RV dysfunction, while in the biventricular failure subgroup, RV dysfunction seemed to be a consequence of higher RV afterload.

Doppler echocardiographic profiles and clinical implications

The hemodynamic profiles by eRAP and eLAP outlined some differences in terms of prognosis, RV function, and treatment (Figure 6). Patients with the optimal unloading profile had better outcomes, while those with high eRAP (both RV failure and biventricular failure profiles) had a higher risk for heart failure.

Figure 6. *Noninvasive Hemodynamic Profiles by the Estep Modified Model*

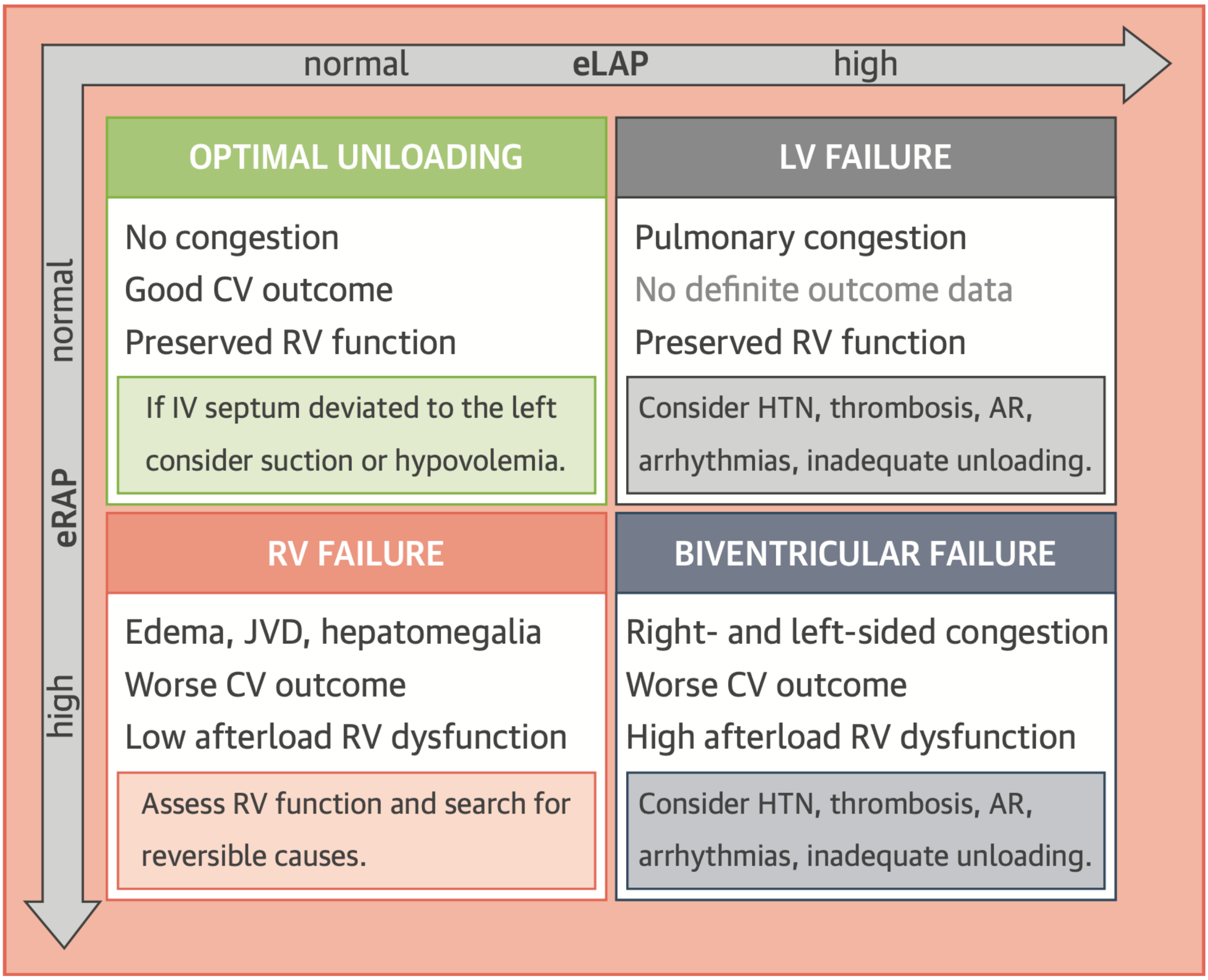

The 4 profiles identified by estimated right atrial pressure (eRAP) and estimated left atrial pressure (eLAP) showed different clinical presentation, outcome, and diagnostics. AR = aortic regurgitation; CV = cardiovascular; HTN = hypertension; JVD = jugular venous distention; RV = right ventricular.

This classification may help clinicians in therapeutic and device management. In case of high WP, hypertension and other specific causes of high LV afterload (e.g., LVAD thrombosis, aortic insufficiency, inadequate unloading) should be considered. An increase in LVAD speed rate may be considered a therapeutic option once other causes are excluded. In case of RV dysfunction, the use of diuretic agents and inotropes may be considered. However, in case of overt primary RV failure, it could be necessary to reduce the LVAD speed and hence to accept suboptimal LV unloading to achieve outpatient stable RV compensation.

Study limitations

The main limits of the study are the monocentric design and the small number of patients enrolled. Even though we collected a wide spectrum of WP and RAP values, an external validation of our algorithm is needed. Also the eLAP Estep modified model, which resulted from a post hoc analysis, lacks a validation cohort.

We collected satisfactory Doppler echocardiographic signals in many patients, but this required the use of off-axis and sometimes atypical sample volume positions and high angles of insonation. Besides, noninvasive estimation was performed by a team with expertise in diastolic evaluation. This could have affected the algorithm accuracy and reproducibility, as Doppler echocardiography is an operator-dependent technique.

Moreover, this study involved only HVAD patients, so the algorithm could not fit other types of LVADs.

The clinical role of noninvasive hemodynamic profiles was not the main goal of the study, and it may have been underpowered to adequately evaluate the association of profiles with different prognosis and treatment. In particular, only 1 patient fit the LV failure profile. The selection of patients implanted (INTERMACS ≤4, mildly dysfunctional right ventricles) may have played a role.

CONCLUSIONS

Noninvasive evaluation of hemodynamic status in HVAD patients by Doppler echocardiography is feasible and reproducible. Both RAP and WP were accurately estimated using a multiparametric approach. High RAP is associated with high WP and adverse outcomes. The benefit of noninvasive evaluation of hemodynamic status in the clinical assessment of LVAD patients should be evaluated.

PERSPECTIVES

COMPETENCY IN MEDICAL KNOWLEDGE: In LVAD patients, noninvasive estimation of high LAP and RAP by Doppler echocardiography is accurate and reproducible and identifies patients with different clinical presentation and prognosis. Furthermore, high RAP was associated with inadequate unloading of the left ventricle and was the strongest predictor of adverse cardiac outcomes.

TRANSLATIONAL OUTLOOK: More studies are needed to assess whether the addition of noninvasive evaluation of hemodynamic status can guide the management of LVAD patients, whether it improves the achievement of optimal unloading of both ventricles, and whether it influences survival and the quality of life of LVAD patients.

REFERENCES

1. Rose EA, Gelijns AC, Moskowitz AJ, et al. Long- term mechanical left ventricular assistance for end-stage heart failure. N Engl J Med 2001;345: 1435–43.

2. Jorde UP, Kushwaha SS, Tatooles AJ, et al., for the HeartMate II Clinical Investigators. Results of the destination therapy post-food and drug administration approval study with a continuous flow left ventricular assist device: a prospective study using the INTERMACS registry (Interagency Registry for Mechanically Assisted Circulatory Support). J Am Coll Cardiol 2014;63:1751–7.

3. Slaughter MS, Pagani FD, McGee EC, et al., for the HeartWare Bridge to Transplant ADVANCE Trial Investigators. HeartWare ventricular assist system for bridge to transplant: combined results of the bridge to transplant and continued access protocol trial. J Heart Lung Transplant 2013;32: 675–83.

4. Horton SC, Khodaverdian R, Chatelain P, et al. Left ventricular assist device malfunction: an approach to diagnosis by echocardiography. J Am Coll Cardiol 2005;45:1435–40.

5. Estep JD, Stainback RF, Little SH, Torre G, Zoghbi WAD. The role of echocardiography and other imaging modalities in patients with left ventricular assist devices. J Am Coll Cardiol Img 2010;3:1049–64.

6. Scalia GM, McCarthy PM, Savage RM, Smedira NG, Thomas JD. Clinical utility of echo- cardiography in the management of implantable ventricular assist devices. J Am Soc Echocardiogr 2000;13:754–63.

7. Lam KM, Ennis S, O'Driscoll G, Solis JM, Macgillivray T, Picard MH. Observations from non-invasive measures of right heart hemodynamics in

left ventricular assist device patients. J Am Soc Echocardiogr 2009;22:1055–62.

8. Topilsky Y, Hasin T, Oh JK, et al. Echocardio- graphic variables after left ventricular assist device implantation associated with adverse outcome. Circ Cardiovasc Imaging 2011;4:648–61.

9. Estep JD, Vivo RP, Krim SR, et al. Echocardio- graphic evaluation of hemodynamics in patients with systolic heart failure supported by a continuous-flow LVAD. J Am Coll Cardiol 2014;64: 1231–41.

10. Shah NR, Cevik C, Hernandez A, Gregoric ID, Frazier OH, Stainback RF. Transthoracic echocar- diography of the HeartWare left ventricular assist device. J Card Fail 2012;18:745–8.

11. Uriel N, Morrison KA, Garan AR, et al. Devel- opment of a novel echocardiography ramp test for speed optimization and diagnosis of device thrombosis in continuous-flow left ventricular assist devices: the Columbia ramp study. J Am Coll Cardiol 2012;60:1764–75.

12. Feldman D, Pamboukian SV, Teuteberg JJ, et al., for the International Society for Heart and Lung Transplantation. The 2013 International So- ciety for Heart and Lung Transplantation Guide- lines for mechanical circulatory support: executive summary. J Heart Lung Transplant 2013;32: 157–87.

13. Lanier GM, Orlanes K, Hayashi Y, et al. Validity and reliability of a novel slow cuff-deflation sys- tem for noninvasive blood pressure monitoring in patients with continuous-flow left ventricular assist device. Circ Heart Fail 2013;6:1005–12.

14. Lang RM, Badano LP, Mor-Avi V, et al. Rec- ommendations for cardiac chamber quantification by echocardiography in adults: an update from the

American Society of Echocardiography and the European Association of Cardiovascular Imaging. J Am Soc Echocardiogr 2015;28:1–39.

15. Zoghbi WA, Enriquez-Sarano M, Foster E, et al. American Society of Echocardiography. Society of Echocardiography. Recommendations for evalua- tion of the severity of native valvular regurgitation with two-dimensional and Doppler echocardiog- raphy. J Am Soc Echocardiogr 2003;16:777–802.

16. Slaughter MS, Pagani FD, Rogers JG, et al. Clinical management of continuous-flow left ventricular assist devices in advanced heart failure. J Heart Lung Transplant 2010;29:S1–39.

17. Rudski LG, Lai WW, Afilalo J, et al. Guidelines for the echocardiographic assessment of the right heart in adults: a report from the American Society of Echocardiography endorsed by the European Association of Echocardiography, a registered branch of the European Society of Cardiology, and the Canadian Society of Echocardiography. J Am Soc Echocardiogr 2010;23:685–713.

18. Frea S, Bovolo V, Bergerone S, et al. Echo- cardiographic evaluation of right ventricular stroke work index in advanced heart failure: a new index? J Card Fail 2012;18:886–93.

19. Kang G, Ha R, Banerjee D. Pulmonary artery pulsatility index predicts right ventricular failure after left ventricular assist device implantation. J Heart Lung Transplant 2016;35:67–73.

20. Kircher BJ, Himelman RB, Schiller NB. Nonin- vasive estimation of right atrial pressure from the inspiratory collapse of the inferior vena cava. Am J Cardiol 1990;66:493–6.

21. Appleton CP, Hatle LK, Popp RL. Demonstra- tion of restrictive ventricular physiology by Doppler echocardiography. J Am Coll Cardiol 1988;11:757–68.

22. Nagueh SF, Kopelen HA, Zoghbi WA. Relation of mean right atrial pressure to echocardio- graphic and Doppler parameters of right atrial and right ventricular function. Circulation 1996; 93:1160–9.

23. Nagueh MF, Kopelen HA, Zoghbi WA, Quinones MA, Nagueh SF. Estimation of mean right atrial pressure using tissue Doppler imaging. Am J Cardiol 1999;84:1448–51.

24. Sade LE, Gulmez O, Eroglu S, Sezgin A, Muderrisoglu H. Noninvasive estimation of right ventricular filling pressure by ratio of early tricuspid inflow to annular diastolic velocity in patients with and without recent cardiac surgery. J Am Soc Echocardiogr 2007; 20:982–8.

25. Tei C, Tanaka H, Kashima T, Yoshimura H, Minagoe S, Kanehisa T. Real-time cross-sectional echocardiographic evaluation of the interatrial septum by right atrium-interatrial septum-left atrium direction of ultrasound beam. Circulation 1979;60:539–46.

26. Mishra RK, Galloway JM, Lee ET, et al. The ratio of mitral deceleration time to E-wave velocity and mitral deceleration slope outper- form deceleration time alone in predicting cardiovascular outcomes: the Strong Heart Study. J Am Soc Echocardiogr 2007;20: 1300–6.

27. Nagueh SF, Smiseth OA, Appleton CP, et al. Recommendations for the evaluation of left ventricular diastolic function by echocardiography: an update from the American Society of Echocardiography and the European Association of Cardio- vascular Imaging. J Am Soc Echocardiogr 2016;29: 277–314.

28. Ritzema JL, Richards AM, Crozier IG, et al. Serial Doppler echocardiography and tissue Doppler imaging in the detection of elevated directly measured left atrial pressure in ambulant subjects with chronic heart failure. J Am Coll Cardiol Img 2011;4:927–34.

29. Morimont P, Lambermont B, Ghuysen A, et al. Effective arterial elastance as an index of pulmo- nary vascular load. Am J Physiol Heart Circ Physiol 2008;294:H2736–42.

30. Frea S, Pidello S, Bovolo V, et al. Prognostic incremental role of right ventricular function in acute decompensation of advanced chronic heart failure. Eur J Heart Fail 2016;18:564–72.

31. Mintz GS, Kotler MN, Parry WR, Iskandrian AS, Kane SA. Real-time inferior vena caval ultraso- nography: normal and abnormal findings and its use in assessing right-heart function. Circulation 1981;64:1018–25.

32. Moreno FL, Hagan AD, Holmen JR, Pryor TA, Strickland RD, Castle CH. Evaluation of size and dynamics of the inferior vena cava as an index of right-sided cardiac function. Am J Cardiol 1984;53: 579–85.

33. Houston BA, Kalathiya RJ, Hsu S, et al. Right ventricular afterload sensitivity dramatically in- creases after left ventricular assist device im- plantation: a multi-center hemodynamic analysis. J Heart Lung Transplant 2016;35:868–76.